

# THERMAL PHASE TRANSITIONS IN FINITE QUANTUM SYSTEMS

D.J. DEAN

*Physics Division, Oak Ridge National Laboratory*

*P.O. Box 2008, MS. 6373, Oak Ridge, TN 37831-6373 USA*

## 1. Introduction

In this Proceedings, I will describe the behavior of two different quantum-mechanical systems as a function of increasing temperature. While these systems are somewhat different, the questions addressed are very similar, namely, how does one describe transitions in phase of a finite many-body system; how does one recognize these transitions in practical calculations; and how may one obtain the order of the transition.

Thermal transitions that may develop in finite systems are somewhat difficult to recognize in practice. Recently Borrmann [1, 2] suggested a method to study these transitions. The method is based on an analysis that Grossmann and Rosenhauer made for macroscopic systems about three decades ago [3]. One evaluates the canonical partition function  $Z(\mathcal{B})$  at complex arguments  $\mathcal{B} = \beta + i\tau$ . Since  $Z(\beta)$  is real, it suffices to consider the partition function  $Z(\mathcal{B})$  for arguments in the upper complex plane. A line of zeros that intersects the real axis at the critical temperature separates two different phases of the macroscopic system. Further information about the order of the phase transition is encoded in the slope of the line at the intersection point and the density of zeros close to the intersection point. This is physically plausible. We recall that thermodynamic quantities are given by logarithmic derivatives of the partition function and thus diverge at its zeros.

In finite systems, the line of zeros reduces to more or less closely spaced zeros that line up on a curve. Following Ref. [1], one then studies the behavior of the zeros with the smallest imaginary part and of the underlying curve while increasing the number of particles. This allows one to predict the critical temperature and order of the phase transition in the infinite system. Furthermore, the shape of the curve or the presence of several such

curves allows one to identify different “phases” already in finite systems. These techniques have been used to study precursors of phase transitions in Bose–Einstein condensates of ideal gases and non-interacting atomic clusters [1, 2]. The order of the phase transition is determined as follows [1]. The distribution of zeros close to the real axis is approximately described by three parameters. Two of these parameters reflect the order of the phase transition, while the third indicates the size of the system. Let us assume that the zeros lie on a line. We label the zeros according to their closeness to the real axis. Thus  $\tau_1$  reflects the discreteness of the system. The density of zeros (DOZ) for a given  $\tau_k$  is given by

$$\phi(\tau_k) = \frac{1}{2} \left( \frac{1}{|\mathcal{B}_k - \mathcal{B}_{k-1}|} + \frac{1}{|\mathcal{B}_{k+1} - \mathcal{B}_k|} \right), \quad (1)$$

with  $k = 2, 3, 4, \dots$ . A simple power law describes the density of zeros for small  $\tau$ , namely  $\phi(\tau) \sim \tau^\alpha$ . If we use only the first three zeros, then  $\alpha$  is given by

$$\alpha = \frac{\ln \phi(\tau_3) - \ln \phi(\tau_2)}{\ln \tau_3 - \ln \tau_2}. \quad (2)$$

The final parameter that describes the distribution of zeros is given by  $\gamma = \tan \nu \sim (\beta_2 - \beta_1)/(\tau_2 - \tau_1)$ .

In the remainder of this Proceedings, I will discuss two systems to which we have applied the DOZ of the partition function. In both systems a two-body interaction is present in contrast to Borrmann’s work. I discuss the melting of the one-vortex state in a Bose-Einstein condensate [4], and phases of a nuclear pairing problem [5] with non-degenerate single-particle spacing.

## 2. Melting of the one-vortex state in a Bose-Einstein condensate

Studies of vortices in dilute atomic Bose–Einstein condensates have received much attention in recent years. The condensate wave function of a vortex state exhibits a quantized circulation of its velocity field. This state may experimentally be formed, e.g., by “phase imprinting” techniques [6] or by directly transferring angular momentum to the condensating system [7]. We address here the regime of long coherence length. Indeed, harmonically trapped Bose systems with perturbatively weak repulsive interactions display a rich structure [8]. At low ratios of angular momentum  $L$  to particle number  $N$ , i.e.  $L/N \ll 1$ , the ground states are dominated by quadrupole and octupole excitations [9, 10] and changes smoothly until the one-vortex state  $L/N = 1$  is approached. The one-vortex state is a Bose–Einstein condensed state where a macroscopic number of particles carries one quantum of angular momentum each [11]. Naturally, the question arises whether the

observed changes in the condensate wave function structure and the formation of quantized vortices are associated with thermal phase transitions.

For the transition to the one-vortex state, the answer is affirmative. Wilkin *et al.* [11] showed that the one-particle reduced density matrix of the one-vortex state has one eigenvalue of order  $N$  and thus meets a criterion for Bose–Einstein condensation in finite systems; see e.g. [12]. The order of this phase transition, however, was not known until now. In this section, I will use the complex zeros of the partition function to classify this phase transition from its precursors in finite systems.

We consider a system of  $N$  bosons confined in a three-dimensional harmonic trap at total angular momentum  $L$  and restrict ourselves to the sector of maximal magnetic quantum number; i.e. the particles are in the ground state with respect to excitations along the axis of rotation. The non-interacting system is highly degenerate. In what follows, we assume that the repulsive interaction between the bosons is perturbatively weak and simply lifts this degeneracy. This yields sets of now quasi-degenerate states that are separated by multiples of the oscillator spacing  $\hbar\omega$ . Under these conditions, the level spacing between quasi-degenerate states is much smaller than the oscillator spacing. We are interested in the thermal properties of the system while keeping the angular momentum  $L$  fixed. For temperatures that are smaller than the oscillator spacing, we may restrict ourselves to the lowest-lying set of quasi-degenerate states with approximate energies  $E \approx L\hbar\omega$ . (We set the ground state energy of the non-rotating system to zero.) Current experiments do not work within this low-temperature regime. We recall that the onset of Bose–Einstein condensation is already observed for temperatures  $kT \sim N^{1/3}\hbar\omega$  [13]. Below we find that quantitative results concerning thermal phase transitions are already determined by a few hundred low-lying levels.

It thus seems that one can lift the requirement of perturbatively small temperatures without facing the inclusion of highly excited states for the problem under consideration. In the low-temperature regime, the Hamiltonian of the  $N$ -boson system with contact interaction reads [14]

$$\hat{H} = v_0 \sum_{i,j,k,l} \frac{(k+l)! \delta_{k+l}^{i+j}}{2^{k+l} (i! j! k! l!)^{\frac{1}{2}}} \hat{a}_i^\dagger \hat{a}_j^\dagger \hat{a}_k \hat{a}_l. \quad (3)$$

Here,  $v_0$  denotes the strength of the contact interaction. The operators  $\hat{a}_j^\dagger$  and  $\hat{a}_j$  create and annihilate one boson in the single-particle state with angular momentum  $j$  with  $j = 0, 1, 2, \dots$ , respectively. The operators  $\hat{N} = \sum_j \hat{n}_j$  and  $\hat{L} = \sum_j j \hat{n}_j$  count the number of particles and the quanta of angular momentum and have quantum numbers  $N$  and  $L$ , respectively. We have used the number operators  $\hat{n}_j = \hat{a}_j^\dagger \hat{a}_j$ . Basis states are denoted

as  $|n_0, n_1, n_2, \dots\rangle$ , where  $n_j$  denotes the number of particles with angular momentum  $j$ .

We investigated the transition to the one-vortex state first. For this purpose, we fix the number of particles to  $N = 30$  and fully diagonalize the Hamiltonian for several values of angular momentum in the range  $0.8 < L/N < 1.07$  around the one-vortex state  $L/N = 1$ . The partition function is computed from the obtained energy levels. We found that the zeros approach the real axis with increasing  $L$ . The closest encounter is found for the one-vortex state  $L = N = 30$ . This is a precursor of the condensation into the one-vortex state in the infinite system and supports earlier results [11, 14, 10]. We are particularly interested in the order of this phase transition. To this purpose, we consider the one-vortex state  $L = N$  and compute eigenvalues of the Hamiltonian (3) for increasing values of particle number  $N$ . A complete diagonalization is prohibitively expensive for  $N$  exceeding values of about 35. Instead, we restrict ourselves to the computation of the lowest-lying eigenvalues. These are used for an approximate construction of the partition function. We found numerically that its zeros with smallest positive imaginary parts are already sufficiently well converged when only a few hundred eigenvalues are included in the computation. We considered systems up to  $L = N = 55$ , corresponding to a dimension of Hilbert space of the order  $4.5 \times 10^5$ . The relevant eigenvalues are computed numerically using the ARPACK and PARPACK routines [15].

Figure 1 shows the distribution of poles in the complex plane of the specific heat at the one-vortex state for different system sizes. These plots are generated from the lowest-lying 300 eigenvalues. (Increasing the number of eigenvalues from 300 to 380 yields less than 1% change in the numerical results. Thus, the data are sufficiently well converged for our purposes.) It is clearly seen that the zeros line up and approach the real axis with increasing system size.

We are now able to classify the transition using the parameters  $\alpha$ ,  $\gamma$ , and  $\tau_1$ , as described in the Introduction. In the thermodynamic limit,  $\tau_1 \rightarrow 0$ , in which case the parameters  $\alpha$  and  $\gamma$  coincide with the infinite system limits discussed by Grossmann and Rosenhauer [3]. For infinite systems,  $\alpha = 0$  and  $\gamma = 0$  indicates a first-order phase transition, while  $0 < \alpha < 1$  and  $\gamma = 0$  or  $\gamma \neq 0$  indicates a second-order transition. For systems approaching infinite particle number,  $\alpha$  cannot be smaller than zero since this causes a divergence of the internal energy. In small systems, with finite  $\tau_1$ ,  $\alpha < 0$  is possible and is also indicative of a first-order transition. We show our results for  $\alpha, \gamma, \tau_1$  in Table 1 for the  $N = 40, 50, 52, 55$  systems.  $\tau_1$  decreases with increasing system size as a power law. The fit is given by  $\tau_1 = 1.15N^{-1.53}$ . From the table, we note that  $\gamma$  is nearly zero, and  $\alpha$  is a small negative

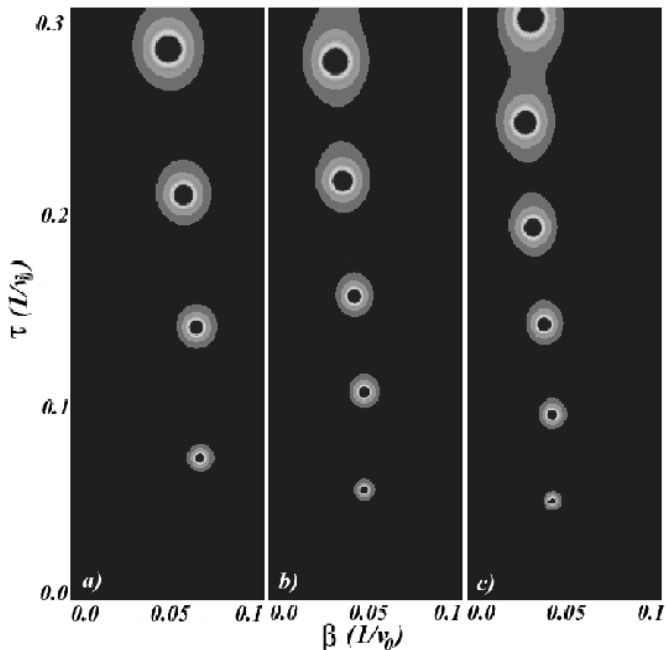


Figure 1. Contour plots of the specific heat in the complex temperature plane for the  $L/N = 1$  systems with increasing numbers of particles: a)  $N = 40$ , b)  $N = 50$ , and c)  $N = 55$ . The spots indicate the locations of the zeros of the canonical partition function.

$N$	$\tau_1$	$\gamma$	$\alpha$
40	0.0715	-0.03	-0.1109
50	0.055	0.0	-0.145
52	0.053	0.003	-0.147
55	0.050	0.003	-0.148

TABLE 1. Calculated parameters  $\tau_1$ ,  $\gamma$ , and  $\alpha$  for the various boson systems at  $L/N = 1$ .

number for each system we studied here. The critical temperature  $kT_c$  is approximately given by  $1/\beta_1$ . Our data suggest that  $kT_c \sim v_0 N^{1.1 \dots 1.4}$ . The  $N$ -dependence differs considerably from what is found for the ideal Bose gas in three-dimensional traps [13].

We thus find that the phase transition to the one-vortex state is first order. This result combines well with previous results found for the energy and wave function structure. We recall that the ground state energy of the

$N$ -boson system exhibits a kink at  $L = N$ , and that the wave function structure changes strongly when increasing  $L$  beyond  $N$  [14, 10].

### 3. Nuclear pairing transitions

We turn now to a fermion problem familiar from nuclear physics. When a system of correlated fermions such as electrons or nucleons is sufficiently small, the fermionic spectrum becomes discrete. If the spacing approaches the size of the pairing gap, superconductivity is expected to break down [16]; however, recent experiments on superconducting ultrasmall aluminum grains by Tinkham *et al.* [17] revealed the existence of a spectroscopic gap larger than the average electronic level density. This feature was interpreted as a reminiscence of superconductivity and renewed the interest [18, 19, 20, 21] in studies of what is the lower size limit for superconductivity.

Other finite fermionic systems such as nuclei are expected to exhibit a variety of interesting phase-transition-like phenomena, like the disappearance of pairing at a critical temperature  $T_c \approx 0.5 - 1$  MeV or the nuclear shape transitions of deformed nuclei associated with the melting of shell effects at  $T_c \approx 1 - 12$  MeV. In recent theoretical and experimental studies [22, 23] of thermodynamical properties of finite nuclei, the heat capacity has been found to exhibit a non-vanishing bump at temperatures proportional to half the pairing gap. These bumps were interpreted as signs of the quenching of pair correlations, representing, in turn, features of the pairing transition for an infinitely large system. Here we will demonstrate the differences among even and odd systems, and strongly paired systems using the DOZ techniques.

Since we are dealing with pairing correlations, we choose our Hamiltonian as

$$H = \sum_i \varepsilon_i a_i^\dagger a_i - G \sum_{ij} a_i^\dagger a_{\bar{i}}^\dagger a_j a_j, \quad (4)$$

where  $a^\dagger$  and  $a$  are fermion creation and annihilation operators, respectively. The indices  $i$  and  $j$  run over the number of levels  $L$ , and the label  $\bar{i}$  stands for a time-reversed state. The parameter  $G$  is the strength of the pairing force, while  $\varepsilon_i$  is the single-particle energy of level  $i$ . We assume that the single-particle levels are equidistant with a fixed spacing  $d$ . Moreover, in our simple model, the degeneracy of the single-particle levels is set to  $2J + 1 = 2$ , with  $J = 1/2$  being the spin of the particle.

For systems with less than  $\sim 16 - 18$  particles, this model can be diagonalized exactly, and we can obtain *all eigenstates*. In our studies below, we will always consider the case of half-filling, i.e., equal number of particles and single-particle levels. This case has the largest dimensionality: for 16 particles in 16 doubly degenerate single-particle shells, we have a total of

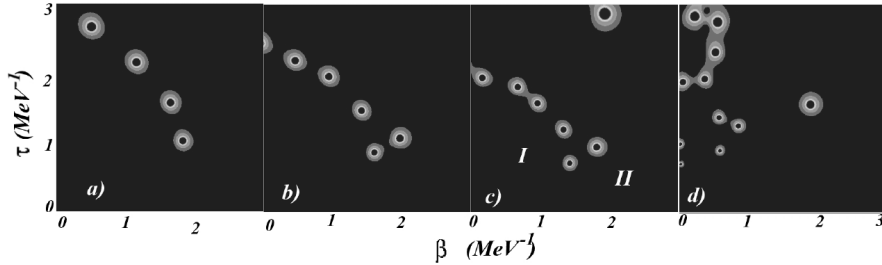


Figure 2. Contour plots of the specific heat in the complex temperature plane for a)  $N = 11$ , b)  $N = 14$ , and c)  $N = 16$  particles. Panel d) shows the  $N = 14$  case with weak pairing. The spots indicate the locations of the zeros of the canonical partition function.

$4 \times 10^8$  states. We choose units MeV for the energy and set  $G = 0.2$  MeV in all calculations while we let  $d$  vary.

In Fig. 2 we show contour plots of the specific heat  $|C_v(\mathcal{B})|$  in the complex temperature plane for  $N = 11$  (a),  $14$  (b), and  $16$  (c) particles at normal pairing  $d/G = 0.5$  and the  $N = 14$  (d) in the weak pairing limit,  $d/G = 2$ . The poles are at the center of the dark contour regions. We see evidence of two phases in these systems. The first phase, labeled *I* in Fig. 2, is a mixed seniority phase, while the second phase, *II*, is a paired phase with zero seniority and exists only in even- $N$  systems. No paired phase exists in the  $N = 11$  system and no clear boundaries are evident in the weak pairing case. The latter also lends support to our microcanonical analysis. For  $d/G > 1.5$ , the free energy develops only one minimum. We find that for (b) and (c) the zeros are apparently distributed along two lines where the intersection occurs at  $\tau_1$ , which is the pole closest to the real axis. As the pairing branch (for  $\beta > \beta_1$ ) only encompasses two points, we are unable to precisely determine  $\alpha$  along this branch while  $\gamma > 0$ . It is therefore not fully clear whether  $\alpha$  along this branch will be positive and thereby allow us to classify the transition as second order. However, the method of Borrmann *et al.* reveals the development of distinct phases.

#### 4. Conclusions

Finite quantum-mechanical systems do not undergo phase transitions; however, one may study the residual effects of phase transitions by analytically continuing the partition function of a given system into the complex plane. We applied this method to a boson system for which we found indications of a first-order transition. In the case of nuclear pairing, we find a phase difference between even and odd systems, although we were not able

to exactly classify it with the DOZ technique. It can be classified using microcanonical-ensemble techniques from which we find that the transition is second order [5]. We will in the future extend these techniques to incorporate more complicated nuclear interactions (such as deformation) to understand their influence on phase transitions.

### Acknowledgements

Oak Ridge National Laboratory is managed by UT-Battelle, LLC for the US Department of Energy under Contract No. DE-AC05-00OR22725. This work is the result of collaborations with A. Belić, M. Hjorth-Jensen, and T. Papenbrock.

### References

1. P. Borrmann, O. Mülken, and J. Harting, Phys. Rev. Lett. **84**, 3511 (2000).
2. O. Mülken, P. Borrmann, J. Harting, and H. Stamerjohanns, Phys. Rev. A **64**, 013611 (2001).
3. S. Grossmann and W. Rosenhauer, Z. Phys. **207**, 138 (1967); **218**, 437 (1969); **218**, 449 (1969).
4. D.J. Dean and T. Papenbrock, submitted to Phys. Rev. A (2001), and arXiv:cond-mat/0107613.
5. A. Belić, D.J. Dean, and M. Hjorth-Jensen, submitted to Phys. Rev. Lett. (2001), and arXiv:cond-mat/0104138.
6. M. R. Matthews, B. P. Anderson, P. C. Haljan, D. S. Hall, C. E. Wieman, and E. A. Cornell, Phys. Rev. Lett. **83**, 2498 (1999).
7. K. W. Madison, F. Chevy, W. Wohlleben, and J. Dalibard, Phys. Rev. Lett. **84**, 806 (2000).
8. D. A. Butts and D. S. Rokhsar, Nature **397**, 327 (1999).
9. B. Mottelson, Phys. Rev. Lett. **83**, 2695 (1999).
10. G. M. Kavoulakis, B. Mottelson, and C. J. Pethick, Phys. Rev. A **62**, 063605 (2000).
11. N. K. Wilkin, J. M. F. Gunn, and R. A. Smith, Phys. Rev. Lett. **80**, 2265 (1998).
12. A. J. Leggett, Rev. Mod. Phys. **73**, 307 (2001).
13. For a review see, e.g., F. Dalfovo, S. Giorgini, L. P. Pitaevskii, and S. Stringari, Rev. Mod. Phys. **71**, 463 (1999).
14. G.F. Bertsch and T. Papenbrock, Phys. Rev. Lett. **83**, 5412 (1999).
15. R. B. Lehoucq, D. C. Sorensen, and C. Yang, *ARPACK Users' Guide: Solution of Large-Scale Eigenvalue Problems with Implicitly Restarted Arnoldi Methods*, SIAM (1998), code available at <http://www.caam.rice.edu/software/ARPACK/>.
16. P. W. Anderson, J. Phys. Chem. Solids **11**, 28 (1959).
17. D. C. Ralph, C. T. Black, and M. Tinkham, Phys. Rev. Lett. **74**, 3241 (1995); C. T. Black, D. C. Ralph, and M. Tinkham, *ibid.* **76**, 688 (1996); *ibid.* **78**, 4087 (1997).
18. F. Braun and J. von Delft, Phys. Rev. Lett. **81**, 4712 (1998).
19. A. Mastellone, G. Falci, and R. Fazio, Phys. Rev. Lett. **80**, 4542 (1998).
20. J. Dukelsky and G. Sierra, Phys. Rev. Lett. **83**, 172 (1999).
21. J. von Delft and D. C. Ralph, Phys. Rep. **345**, 61 (2001).
22. S. Liu and Y. Alhassid, preprint nucl-th/0009006 and Phys. Rev. Lett., in press.
23. E. Melby *et al.*, Phys. Rev. Lett. **83**, 3150 (1999); A. Schiller *et al.*, Phys. Rev. C **63**, 021306 (2001); E. Melby *et al.*, *ibid.* **63**, 044309 (2001).